Royal Norwegian Council
for Scientific and Industrial Research
(NTNF)

NORSAR

NORSAR Scientific Report No. 2-88/89

Semiannual Technical Summary

1 October 1988 – 31 March 1989

L.B. Loughran (ed.)

Kjeller, July 1989

VII. SUMMARY OF TECHNICAL REPORTS / PAPERS PUBLISHED

VII.1 Yield determination of Soviet underground nuclear explosions at the Shagan River Test Site

Introduction

The signing of the Threshold Test Ban Treaty (TTBT) by the United States and the Soviet Union in 1974, which limits the size of underground nuclear explosions, focused attention on methods for estimating the size of explosions. Since 1974, considerable research efforts have been devoted to developing various methods of yield estimation, and much progress has been achieved. Reviews of some of these developments may be found in the report OTA-ISC-361 (1988) published by the U.S. Congress, Office of Technology Assessment, and by Bache (1982), Heusinkveld (1982), Lamb (1988) and Storey et al (1982).

In this paper, we focus on the problem of determining yields by teleseismic methods for a set of explosions conducted at the Shagan River test site near Semipalatinsk, USSR. We have analyzed all the events reported by the ISC or NEIC to have occurred at this site between 1965 and 1988, a total of 96 events. As a basis for the yield estimation we have used body-wave magnitude (m_b) determined from global network data as well as two additional explosion source size estimators. The first additional method is the long-term level of the reduced displacement potential, Ψ_∞, which in this paper is measured from the initial explosion-generated P pulse recorded at four UK array stations. The second additional method is based on estimating the energy of the Lg wave train recorded at the NORSAR and Gräfenberg arrays for each explosion. The emphasis of the paper is on assessing the combined utility of these three methods to obtain relative yields of explosions, but we will also briefly address the estimation of absolute yields from the available seismic information.

The Shagan River test site

The principal Soviet testing area for nuclear explosions is located near the city of Semipalatinsk in Eastern Kazakhstan. Marshall, Bache and Lilwall (1985) identify three distinct test sites within this area: Shagan River, Degelen Mountains and Konystan. After 1976, all of the largest Soviet nuclear tests have been conducted at the Shagan River site, and our discussions in this paper will focus on this area.

A review of available information on the tectonics and geology of the Eastern Kazakhstan area can be found in Leith (1987). Geologically, he describes the test area as located within the Kazakh fold system, which is a complex of deformed Paeozoic rocks along the eastern edge of the so-called "Kazakh shield". Seismically, the region is characterized by relatively modest earthquake activity, but it is noteworthy that some of the explosions at the Shagan River test site have been accompanied by a significant amount of tectonic release (Helle and Rygg, 1984; Given and Mellman, 1986).

A map summarizing the surface geology of the Shagan River area is shown in Fig. VII.1.1. This map is based on imagery from the SPOT satellite as well as information available from the literature (Sukhonikov, Akhmetov and Orlov, 1973; Izrael, 1972; Peyre and Mossakovsky, 1982). A particularly noteworthy feature is the presence of two approximately parallel faults extending across parts of the test site. One of these, the Chinrau fault, appears to show evidence of recent offset on SPOT imagery to the region northwest of Shagan River (Leith, 1987).

Also identified from the satellite observations, and indicated on Fig. VII.1.1, is a crater formed by the explosion of 15 January 1965. This location has been used as a reference point in the relocation of explosions in the test area (Marshall et al, 1985), using the Joint Epicenter Determination method described by Douglas (1967). In the further analysis presented in this paper, we will refer to epicenters calculated from this procedure to the extent such data area available.

Data base

The data base for this study consists of seismic recordings for 96 presumed nuclear explosions at the Shagan River test area, occurring from 1965 through 1988 and located by the ISC or NEIC.

Data sources are the four UK array stations: (Eskdalemuir (ESK), Scotland, Yellowknife (YKA), Canada, Gauribidanur (GBA), India, and Warramunga (WRA), Australia, in addition to the two large arrays NORSAR in Norway and Gräfenberg (GRF) in the Federal Republic of Germany.

The four UK arrays have been in operation since the mid-1960s and are described in detail by Mowat and Burch (1977). Briefly, these are medium-aperture arrays (10-30 km diameter), with 19 or 20 vertical-component Willmore SP seismometers deployed in two roughly perpendicular lines. Their outputs are recorded on analog or digital magnetic tape. The sampling rate, for both digitally recorded data and digitized analog data, is 20 samples per second.

The NORSAR array (Bungum, Husebye and Ringdal, 1971) was established in 1970, and originally comprised 22 subarrays, deployed over an area of 100 km diameter. Since 1976 the number of operational subarrays has been 7, comprising altogether 42 vertical-component SP sensors (type HS-10). In this paper, analysis has been restricted to data from these 7 subarrays. Sampling rate for the NORSAR SP data is 20 samples per second, and all data are recorded on digital magnetic tape.

The Gräfenberg array (Harjes and Seidl, 1978) was established in 1976, and today comprises 13 broadband seismometer sites, three of which are 3-component systems. The instrument response is flat to velocity from about 20 seond period to 5 Hz. Sampling rate is 20 samples per second, and the data are recorded on digital magnetic tape.

Source size estimators

Network m_b magnitude

Body-wave magnitudes averaged over a well-distributed global network have traditionally been the most commonly used measure for yield estimation purposes. In recent years the maximum-likelihood technique (Ringdal, 1976; Christoffersson, 1980) has become widely accepted as a means to obtain m_b estimates that avoid bias due to detection threshold characteristics at individual network stations.

Maximum-likelihood m_b for the explosions in the present data base have been computed at Blacknest applying the method of Lilwall, Marshall and Rivers (1988). Note that this method uses a standardized set of stations and includes individual station corrections for the Shagan River area. The station observations given in the Bulletin of the ISC have been used in these computations, except for events after 1986, where the data have been obtained from the NEIC monthly earthquake data report.

Reduced displacement potential, Ψ_∞

The reduced displacement potential $\Psi(t)$ is a convenient mathematical description of the source function of an explosion, assuming a spherical wave in an ideal, infinite homogeneous, isotropic elastic solid. It is directly related to the moment function $M_0(t)$ of the explosion as follows (Mueller, 1973):

$$M_0(t) = 4\Pi \rho v_p^2 \Psi(t) \quad (1)$$

where ρ is the density of the medium and v_p is the compressional wave velocity.

The long-term (static) level of $M_0(t)$ is often denoted the seismic moment of the explosion, and is a measure of the seismic source size.

Thus, the long-term level of $\Psi(t)$, Ψ_∞, can be used to estimate source size, assuming that the source material properties are known.

The method used in this paper for estimating Ψ_∞ is based on UK array data and has been described in detail by Stewart (1988).

Lg magnitude

The seismic Lg wave propagates in the continental lithosphere and can be observed from large explosions as far away as 5000 km in shield and stable platform areas (Nuttli, 1973; Baumgardt, 1985). Lg is generally considered to consist of a superposition of many higher-mode surface waves of group velocities near 3.5 km/s, and its radiation is therefore expected to be more isotropic than that of P waves. Thus, full azimuthal coverage is not essential for reliable determination of Lg magnitude. Furthermore, Lg is not affected by lateral heterogeneities in the upper mantle, which can produce strong focussing/defocussing effects on P-waves, and therefore contribute to a significant uncertainty in P-based m_b estimates.

Nuttli (1986a) showed that the amplitudes of Lg near 1 second period provide a stable estimate of magnitude, m_b(Lg) and explosion yield for Nevada Test Site explosions. He also applied his measurement methods to Semipalatinsk explosions (Nuttli, 1986b), using available WWSSN records to estimate m_b(Lg) and yields of these events.

Ringdal (1983) first suggested a method to determine Lg magnitudes based on digitally recorded array data. The main idea was to improve the precision of such estimates by averaging over time (computing RMS values over an extended Lg window), frequency (using a bandpass filter covering all frequencies with significant Lg energy) and space (by averaging individual array elements). The method, which can also be used for P coda magnitude estimation, has been described by Ringdal and Hokland (1987) and Ringdal and Fyen (1988).

Data analysis

Results from applying the analysis methods described in the preceding section are summarized in Table VII.1.1. The following comments apply:

Origin times and epicentral information of each event are those calculated at Blacknest using ISC and NEIC data for events up to and including 1985, and are taken from NEIC listings for later events. The magnitude (m_b) values have been computed as earlier described.

For each event an indicator is given corresponding to a subdivision of the Shagan River area into three main areas. These are defined by the two faults marked on Fig. VII.1.1 and an assumed prolongation of the stippled lines indicated on that figure. The three areas are denoted "NE" (Northeast), "TZ" (transition zone between the faults) and "SW" (Southwest), respectively.

Estimates of log Ψ_∞ in Table VII.1.1 are network averages using UK array data. The number of stations available and standard deviations of the estimates are listed for each event. Individual array measurements for most of the events may be found in Stewart (1988).

NORSAR and Gräfenberg (GRF) Lg magnitude estimates are noise-corrected array averages, obtained by applying individual bias corrections for each array element. The number of operative array channels are given for each event. Standard deviations of the array averages have been computed taking into account both the number of sensors and the signal-to-noise ratios (for details, see Ringdal and Fyen, 1988). Estimates have been made for all events for which array recordings were available, except those with too low Lg signal-to-noise ratio to allow reliable measurement. Table VII.1.1 also contains weighted averages (discussed later in this section) of the NORSAR and GRF Lg magnitudes.

The Lg magnitude estimates in Table VII.1.1 are, except for a few minor revisions, consistent with those presented in earlier Semiannual Reports. We have not included corrections for epicentral distance differences in this paper, since these are small to begin with, and also difficult to estimate accurately given the limited knowledge of local attenuation in the Shagan River area.

As noted by Ringdal and Fyen (1988), the Lg array estimates at NORSAR and Gräfenberg may be made with very high precision, due to the large number of channels (up to 42 and 13, respectively). Thus, the standard deviation across NORSAR of individual measurements is typically 0.07 magnitude units for uncorrected data, and 0.035 units when individual channel corrections are applied. The precision of NORSAR averages are thus better than 0.01 units for high SNR events, but somewhat poorer at lower SNR. At Gräfenberg, the standard deviation of the mean values is typically 2-3 times that of NORSAR, depending on the number of available channels. It should be noted that this high precision does not necessarily imply a correspondingly high degree of accuracy in estimating Lg source energy since the effects of near-source geology remain unknown.

In the comparison which follows of the various source size estimators, we will in particular focus on the subdivision of the Shagan River site into apparently geophysically distinct subregions. Marshall et al (1985) discuss this feature in detail, showing that explosions in the northeast and southwest portions of the test site produce distinctly different P waveforms when recorded at the UK arrays. We note that their northeast region also includes the area denoted by us as a transition zone (TZ). We will pursue this subdivision further by analyzing the differences between P-based and Lg-based magnitude measurements, and later discuss the implications for yield estimation.

Figs. VII.1. 5 through VII.1.8 are scatter plots comparing pairs of source size estimators. In all these figures, we use the following symbols for the three subareas: open squares (SW), filled squares (NE) and crosses (TZ).

We first compare the two P-based estimators, m_b and $\log\Psi_\infty$. Fig. VII.1.2 shows that they are quite consistent, with no systematic difference between the SW, TZ and NE events. In assessing the scatter in this plot, we must take into account that many of the Ψ_∞ estimates are based on data from only one or two arrays (Table VII.1.1).
The least-squares fit to this data set, assuming no errors in m_b, is:

$$\log \Psi_\infty = 1.1\ m_b - 2.57 \qquad (\pm\ 0.11) \qquad (2)$$

where the standard deviation of 0.11 refers to the set of residuals in $\log \Psi_\infty$ relative to the straight line fit.

We next compare the two Lg-based measurements. Fig. VII.1.3 shows a scatter plot of NORSAR versus GRF Lg magnitudes for all events (54) measured at both arrays. The straight line represents a least squares fit to the data, assuming no errors in NORSAR magnitudes, and is given by

$$m_{Lg}(\text{GRF}) = 1.15 \cdot m_{Lg}(\text{NORSAR}) - 0.90 \qquad (\pm\ 0.042) \qquad (3)$$

We note that the two arrays show excellent consistency, although there is some increase in the scattering at low magnitudes. There is no significant separation between events from NE, TZ and SW areas with regard to the relative Lg magnitudes observed at the two arrays.

Fig. VII.1.4 shows a subset of these data (35 events), using only events for which we have the most reliable Lg estimates (at least 6 stations for each array, and estimated standard deviation of m_{Lg} less than 0.04). We note that the scatter is significantly reduced (the standard deviation in the vertical direction is now only 0.031 units, compared to 0.042 units for the entire data set), thus emphasizing the excellent consistency between NORSAR and Gräfenberg.

The slope (1.15) of the straight-line fit in Figs. VII.1.3 and VII.1.4 is slightly greater than 1.00, a tendency also noted by Ringdal and Fyen (1988). The interpretation of this observation is somewhat uncertain; a possible explanation is scaling differences in the Lg source spectrum (Kværna and Ringdal, 1988), in combination with the response differences of the NORSAR and GRF instruments. It is interesting in this connection to note that Patton (1988) observed significant differences between stations in slopes for M(Lg) versus yield, when studying a network of stations recording Nevada Test Site explosions.

In the comparison which follows of P and Lg-based magnitudes, we find it convenient to use as reference a weighted average of the NORSAR and GRF Lg magnitudes. This average is obtained by first using equation (3) to adjust the GRF values to "equivalent" NORSAR magnitudes, and then use the inverse variance obtained from Table VII.1.1 as weighting factors in the averaging procedure. The resulting values, which we denote m_{Lg}, are listed as the rightmost column in Table VII.1.1.

In Fig. VII.1.5, m_b is plotted versus m_{Lg} defined above for all events with both measurements available. Three lines, with slopes restricted to 1.0, have been drawn, representing the three subregions. To obtain improved reliability in calculating the intercepts, we have in that calculation used only events of $m_{Lg} \geq 5.5$, and required that NORSAR Lg measurements are available. The resulting relationships are:

SW region: $m_b = m_{Lg} + 0.05$ ($\pm$ 0.041) (4a)

TZ region: $m_b = m_{Lg} - 0.02$ ($\pm$ 0.031) (4b)

NE region: $m_b = m_{Lg} - 0.10$ ($\pm$ 0.047) (4c)

Taking into account the number of observations in each group, the average bias estimates ($m_b - m_{Lg}$) and their precisions are: 0.05 $\pm$ 0.007 (SW region), - 0.02 $\pm$ 0.009 (TZ region) and - 0.10 $\pm$ 0.012 (NE region). In light of the low standard deviations, the differences in bias values are highly significant, and we note that the NE and SW regions differ by as much as 0.15 magnitude units in this regard.

Fig. VII.1.6 shows a plot of m_{Lg} versus "adjusted" m_b, using the regional correction factors given above. We note that the consistency is excellent, although there are two outliers in the plot (Events 25 and 28 of Table VII.1.1). Event 25 is small, and both the m_b and m_{Lg} measurements for this event are uncertain. Event 28 has an m_{Lg} measurement based on only 3 GRF channels, with no NORSAR data available, and is therefore less precisely determined than the majority of data points. The standard deviation of the m_b-m_{Lg} differences in Fig. VII.1.6 is 0.050 magnitude units, which is reduced to 0.039 units if the two outliers are disregarded.

Fig. VII.1.7 shows a comparison of m_{Lg} to log Ψ_∞ observations. We note a tendency for the SW events to exhibit relatively larger values of log Ψ_∞ than events from the other two regions. However, this bias is less pronounced than that previously observed for m_b versus m_{Lg}. Partly, this is due to increased scatter in the data, since the log Ψ_∞ measurements are based only on a few observations. Nevertheless, it would appear that log Ψ_∞ is less sensitive than m_b to regional bias effects. This can be explained by the longer wavelengths used in log Ψ_∞ measurements in combination with the fact that log Ψ_∞ to a large extent avoids the pP contamination that may adversely influence m_b measurements.

Requiring at least 3 individual array measurements for log Ψ_∞, and using a slope of 0.9 suggested from Fig. VII.1.2 and the general consistency between m_b and m_{Lg}, we obtain the following two relations (marked on the figure)

$$\text{SW} : m_{Lg} = 0.9 \cdot \log \Psi_\infty + 2.35 \quad (\pm 0.05) \qquad (5a)$$

$$\text{NE and TZ} : m_{Lg} = 0.9 \cdot \log \Psi_\infty + 2.43 \quad (\pm 0.075) \qquad (5b)$$

Note that the NE and TZ regions have been grouped together in this case, as we in our analysis have not been able to identify any systematic differences for this data set.

Fig. VII.1.8 shows magnitude differences m_b-m_{Lg} plotted as a function of event location, using only events of $m_b \geq 5.5$ and requiring NORSAR Lg data to be available. The subdivision of the test site as earlier discussed is marked on the figure. The systematic differences, in particular between the NE and SW parts of the test site, are clearly seen. If we attempt to explain this anomaly as resulting from the systematic differences in P recordings only, we obtain a relative m_b(P) bias of about 0.15 m_b units between these two areas. We consider this a realistic interpretation, since it is well known that P-waves are subject to strong focusing effects in the upper mantle, both underneath the source and the receiver. However, the possibility of an m_b(Lg) bias contributing to the mentioned difference cannot be entirely ruled out.

Yield estimation

Yield of the 15 January 1965 explosion

Determination of the appropriate <u>absolute</u> magnitude-yield relationship for explosions at a specific test site requires knowledge of the true yields and testing conditions of some number of representative explosions at that particular site. In the case of the Shagan River nuclear test site, thus far, there has been a discussion in the literature of the yield of only one explosion. This explosion was conducted on 15 January 1965 within the Soviet Peaceful Nuclear Explosion program for the purpose of constructing a reservoir.

We have reviewed available data on this explosion, and obtained a yield estimate which we will use in calibrating the various magnitude-yield relationships. Clearly, in the absence of more detailed calibration data, the relationships will have a significant uncertainty. This applies especially in the absolute yield levels, whereas the <u>relative</u> yield estimates between explosions will be somewhat better constrained.

In IAEA proceedings, the yield of the 1965 explosion is quoted as "above 100 kt". Myasnikov et al (1970) indicates that the scaled apparent radius is 51 $m/kt^{1/3.4}$, which for a crater radius of 204 m gives a yield of 111 kt. Myasnikov et al (1970) uses a scaled depth of burst for this explosion equal to 50 $m/kt^{1/3.4}$. The depth of emplacement is reported to be 200 m (Kedrovskiy, 1970; Izrael, 1972; Myasnikov et al, 1970), which corresponds to the same yield estimate. For the purposes of the work presented here, the yield of the 15 January 1965 explosion is taken to be 111 kt.

Available seismic data

Turning now to the question of relating this yield to the observed data, we first note that the 1965 explosion differs from all the other explosions in our data base by not being fully contained. This means that the interference effects between P and pP will be different for this event and the others.

Our Ψ_∞ measurements rely on the characteristics of the initial positive P-pulse of the explosion, and are therefore less affected by the free surface reflection. However, our m_b estimate of the 15 January 1965 explosion is likely biased low. The actual bias may, from theoretical considerations, typically approach 0.1-0.2 m_b units (Marshall et al, 1979; McLaughlin et al, 1988).

We have reviewed available data for 46 Shagan River explosions recorded at EKA, comparing the maximum peak-to-peak amplitude (c) (the phase which is normally used for magnitude estimation) and the initial zero-to-peak amplitude (a). The average values of $r = \log (c/a)$ for contained explosions were 0.78 (SW), 0.77 (TZ) and 0.72 (NE), with an overall mean of $r = 0.75$. The corresponding value for the 15 January 1965 explosion was $r = 0.62$.

Assuming that the initial pulse is unaffected by pP, this would suggest that a correction factor of about 0.13 m_b units would be appropriate. Since the uncorrected m_b value for the 1965 explosion was 5.87, we consequently obtain an estimated m_b value of 6.00 for a contained explosion of the same size as the 15 January 1965 event. We note that McLaughlin et al (1988) obtained a similar correction factor (0.13) based on theoretical considerations, whereas their observational data indicate a slightly higher value of 0.16 (McLaughlin, personal communcation).

No Lg measurements are available for NORSAR or GRF for the 1965 event. Nuttli (1986b) estimates m_{Lg} = 5.87 for this explosion, but we note that his estimates for events before 1979 tend to be lower (by 0.08 magnitude units on the average) than NORSAR m_{Lg} observations, and his value would therefore correspond to a NORSAR m_{Lg} of about 5.95.

Magnitude-yield relationship

Our basic assumption will be that m_{Lg}, as a yield estimator, is largely independent of the geological variations within the Shagan River test site. This suggests that a single yield-magnitude relationship would be appropriate, and we ill in the following assume a relation of the form

$$m_{Lg} = 0.9 \log Y + k \qquad (6)$$

where k will be estimated using data from the 15 January 1965 explosion. The slope of 0.9 in (6) is consistent with our previous relations between log Ψ_∞, m_b and m_{Lg}, taking into account that log Ψ_∞ has previously been found to scale to logY with a slope of 1 (Stimpson, 1988; Gillbanks et al, 1989).

Since the NORSAR or GRF m_{Lg} for the 15 January 1965 explosion is not known, we need to estimate it indirectly, and then insert the value in (6) for Y = 111 kt in order to obtain an estimate of k. For this purpose, we use the previously discussed estimates of m_b, log Ψ_∞ and m_{Lg} (Nuttli), with the proper adjustments for regional and other bias factors.

(i) For m_b, the value of 6.00 for an explosion in the TZ region corresponds (by 4b) to $m_{Lg} = 6.02$.

(ii) For log Ψ_∞, the value of 3.87 in the TZ region corresponds (by 5b) to $m_{Lg} = 5.91$.

(iii) For Nuttli's m_{Lg}, the value of 5.87 corresponds, as earlier mentioned, to NORSAR $m_{Lg} = 5.95$.

The average (5.96) of these three values is then taken as our best estimate of m_{Lg} for a fully contained explosion of Y = 111 kt. Inserted in (6), this gives k = 4.12, i.e.:

$$m_{Lg} = 0.9 \log Y + 4.12 \qquad (7)$$

In line with our previous considerations, the formula (7) will then be applicable to the entire test site and this enables us to estimate yields for all explosions for which m_{Lg} has been determined.

Supplementary yield estimates from m_b and log Ψ_∞ can now be calculated by using (7) in conjunction with the regionally based formulas (4a-c) and (5a-b).

We obtain, by direct substitution for m_b:

SW region : $m_b = 0.9 \cdot \log Y + 4.17$ (8a)

TZ region : $m_b = 0.9 \cdot \log Y + 4.10$ (8b)

NE region : $m_b = 0.9 \cdot \log Y + 4.02$ (8c)

and for log Ψ_∞:

SW region : $\log \Psi_\infty = \log Y + 1.97$ (9a)

NE and TZ regions : $\log \Psi_\infty = \log Y + 1.88$ (9b)

We note that the constant terms in equations (9a-b) are between the values earlier determined for water-saturated rock at the Nevada Test Site (Gillbanks et al, 1989) and granite at the French test site in S. Algeria (Stimpson, 1988), which were 1.8 and 2.0, respectively.

Table VII.1.2 summarizes yield estimates of individual Shagan River explosions, using the formulas developed earlier. Both P and Lg-based estimates are listed, together with their (logarithmic) average value for each event. The P-based yields represent a weighted average between m_b and log Ψ_∞ estimates, using the inverse variances as weighting factors. Here, we use for log Ψ_∞, the standard deviations listed in Table VII.1.1, and for m_b a standard deviation of 0.04, which is the average of the deviations relative to NORSAR m_b(Lg) within each of the three regions.

Discussion

A method, combining several measurements of the radiated seismic energy of underground nuclear explosions, has been developed which offers the possibility for precise yield estimates in a relative sense. A reliable assessment of the results presented here would require access to independently measured yields, which, with the exception of the data on the 1965 explosion given here, currently is not available. We note, however, that the yield estimate quoted by Sykes and Ekström (1989) of 115-122 kt for the explosion of 9/14/88 compares closely with the values of 113-117 kt derived independently in this study.

It has been noted in this paper that the estimation of the <u>absolute</u> values of the yields by the method presented here relies on knowledge of the yield and geophysical conditions of a single explosion. The estimation of <u>absolute</u> yields by this method relies on a number of critical assumptions, including the assumption that the yield value taken in this study is the appropriate yield, the assumption of correcting the bodywaves for depth of burial effects, the assumption of the equivalent Lg value of the 1965 explosion, and the assumption that the corrected magnitude values for the 1965 explosion are representative of explosions in that area. Incorrect assumptions in these areas would lead to different yield estimates than those given in Table VII.1.1. For instance, a 10% increase in the assumed yield of the 1965 explosion would result in a 10% increase in the predicted yields in Table VII.1.1.

Our measurements on Ψ_∞ show general consistency with maximum likelihood m_b estimates from a global network, and have the advantage of requiring only a few stations for reliable measurement. Furthermore, the associated estimates of P-pulse rise time and duration provide important information related to source corner frequency and near-source geology. These parameters, as discussed by Stewart (1988), are useful for identifying systematic differences between the NE and SW Shagan areas, although determining the source of these differences would require more information on site geology than is currently available.

The m_{Lg} measurements presented in this paper, based on NORSAR and Gräfenberg array recordings, show excellent promise to provide very precise relative yields of individual explosions, but would again require calibration data to determine more reliably the absolute yields. Part of the reasons for this high precision lies in the fact that our Lg magnitudes, as discussed before, are based on averaging the observed Lg signals both in time, frequency and space. The basic assumption is that Lg generation at the source is largely azimuth independent and also independent of local variations in geology.

Because of the large distances (more than 4000 km) from Semipalatinsk to NORSAR and Gräfenberg, reliable measurements of Lg magnitudes can only be made at these arrays for explosions of approximately $m_b = 5.5$ or greater. This corresponds to about 30-40 kilotons for fully coupled explosions, depending on the location within the test site. In order to apply the method to smaller events, seismograph stations at shorter epicentral distances, with good Lg propagation paths, must be available. Again, each station must be individually calibrated in order to obtain reliable estimates.

This paper has demonstrated that observations from three distinct subregions of the Shagan site show systematic differences, supporting and extending earlier studies (e.g., Marshall et al, 1985), suggesting that the NE and SW areas are characterized by different geophysical properties. In particular, the P-Lg magnitude bias shows systematically different behavior for these regions.

This variation, as illustrated in Fig. VII.1.8, is in fact quite smooth, and indicates a knowledge of precise epicenter location would make possible, through interpolation, to obtain an estimate of P-Lg bias also for events for which Lg magnitudes are not available. Such events could be low-magnitude explosions, "double" explosions (for which Lg magnitude would represent the combined yields), explosions followed by large earthquakes causing interference with the Lg wavetrain or events occurring during outage times for the stations reporting Lg measurements.

It is noted that the current bilateral negotiations on nuclear testing offer the possibility for validated yields of future explosions at the Shagan River nuclear test site. Such additional yield information is invaluable in testing, and modifying if necessary, the teleseismic yield estimation method developed in this report.

F. Ringdal
P.D. Marshall, MOD PE, UK

References

Bache, T.C. (1982): Estimating the yield of underground nuclear explosions, Bull. Seism. Soc. Am., 72, S131-S168.

Baumgardt, D.R. (1985): Comparative analysis of teleseismic P coda and Lg waves from underground explosions in Eurasia, Bull. Seism. Soc. Am., 75, 1413-1433.

Bungum, H., E.S. Husebye and F. Ringdal (1971): The NORSAR array and preliminary results of data analysis, Geophys. J., 25, 115-126.

Christoffersson, A. (1980): Statistical models for seismic magnitude, Phys. Earth Planet. Inter., 21, 237-260.

Douglas, A. (1967): Joint epicentre determination, Nature, 215, 47-48.

Gillbanks, T.G.A., P.D. Marshall and R.C. Stewart (1989): P-wave seismograms recorded at Yellowknife, Canada from underground nuclear explosions in Nevada, USA, AWE Report No. 0 26/88, HMSO, London.

Given, J.W. and G.R. Mellman (1986): Estimating explosion and tectonic release source parameters of underground nuclear explosions from Rayleigh and Love wave observations. Final Report, Part 1, SGI-R-86-126 (Sierra Geophysics, Kirkland, WA), 1-70.

Harjes, H.-P. and D. Seidl (1978): Digital recording and analysis of broadband seismic data at the Gräfenberg (GRF) array, J. Geophys. Res., 44, 511-523.

Helle, H.B. and E. Rygg (1984): Determination of tectonic release from surface waves generated by nuclear explosions in eastern Kazakhstan, Bull. Seism. Soc. Am., 74, 1883-1898.

Heusinkveld, M. (1982): Analysis of shock wave arrival time from underground explosions, J. Geophys. Res., 87, 1891-1898.

Izrael, Yui.A. (1972): Phenomenology of the containment of the atmosphere and ground by the radioactive products of underground nuclear explosions, IAEA-388-3/23, Vienna.

Kedrovski, O.L. (1970): The application of contained nuclear explosions in industry. (In Russian with English abstract). In: Peaceful Nuclear Explosions Phenomenology and Status Report, 1970, IAEA, Vienna, 163-185.

Kværna, T. and F. Ringdal (1988): Spectral analysis of Shagan River explosions recorded at NORSAR and NORESS, In: Semiann. Tech. Summ. 1 Apr - 30 Sep 88, NORSAR Sci. Rep. 1-88/89, Kjeller, Norway.

Lamb, F.K. (1988): Monitoring yields of underground nuclear tests using hydrodynamic methods, Nuclear Arms Technology in the 1990s, American Institute of Physics Publications, D. Schroeer and D. Hafmeister (eds.)

Leith, W. (1987): Tectonics of eastern Kazakhstan and implications for seismic source studies in the Shagan River area, In: Papers presented at the 9th Annual DARPA/AFGL Seismic Research Symposium, 15-18 June 1987, 34-37.

Lilwall, R.C., P.D. Marshall and D.W. Rivers (1988): Body wave magnitudes of some underground nuclear explosions at the Nevada (USA) and Shagan River (USSR) test sites, AWE Report No. 0 15/88, HMSO, London.

Marshall, P.D., T.C. Bache and R.C. Lilwall (1985): Body wave magnitudes and locations of Soviet underground explosions at the Semipalatinsk test site, AWRE Report No. 0 16/84 (re-issue), HMSO, London.

Marshall, P.D., D.L. Springer and H.C. Rodean (1979): Magnitude corrections for attenuation in the upper mantle, Geophys. J.R. astr. Soc., 5, 609-638.

McLaughlin, K.L., T.G. Barker, S.M. Day, B. Shkoller and J.L. Stevens (1988): Effects of depth of burial and tectonic strain release on regional and teleseismic explosion waveforms, Report No. AFGL-TR-88-0314, S-CUBED, La Jolla, California.

Mowat, M.W.H. and R.F. Burch (1977): Handbook for the stations which provide seismograms to the Blacknest Seismological Centre, United Kingdom, AWRE Blacknest Tech. Rep. 44/47/29 Blacknest, Brimpton, RG7 4RS, UK.

Mueller, G. (1973): Seismic moment and long period radiation of underground nuclear explosions, Bull. Seism. Soc. Am., 63, 847-858.

Myasnikov, K.V., L.B. Prozorov and I.E. Sitnikov (1970): Mechanical effects of single and multiple underground nuclear cratering explosions and the properties of the excavation dug by them, In: Nuclear Explosions for Peaceful Purposes, Ed. I.D. Morokhov (Atomizdat, Moscow), LLL Report UCRL-Trans-10517, 79-109.

Nuttli, O.W. (1973): Seismic wave attenuation and magnitude relations for eastern North America, J. Geophys. Res., 78, 876-885.

Nuttli, O.W. (1986a): Yield estimates of Nevada test site explosions obtained from seismic Lg waves, J. Geophys. Res., 91, 2137-2151.

Nuttli, O.W. (1986b): Lg magnitudes of selected East Kazakhstan underground explosions, Bull. Seism. Soc. Am., 76, 1241-1251.

Office of Technology Assessment, U.S. Congress (1988): Seismic Verification of Nuclear Testing Treaties, GPO, Washington, D.C., Report OTA-ISC-361, 1-139.

Patton, H.J. (1988): Application of Nuttli's method to estimate yield of Nevada test site explosions recorded on Lawrence Livermore National Laboratory's digital seismic system, Bull. Seism. Soc. Am., 78, 1759-1772.

Peyre, A.V. and A.A. Mossakovsky (1982): Tectonics of Kazakhstan, In: Exploratory Report for Tectonic Map of Kazakhstan, Nauka, Moscow.

Ringdal, F. (1976): Maximum-likelihood estimation of seismic magnitude, Bull. Seism. Soc. Am., 66, 789-802.

Ringdal, F. (1983): Magnitudes from P coda and Lg using NORSAR data, In: NORSAR Semiann. Tech. Summ., 1 Oct 1982 - 31 Mar 1983, NORSAR Sci. Rep. 2-82/83, Kjeller, Norway.

Ringdal, F. and B.Kr. Hokland (1987): Magnitudes of large Semipalatinsk explosions using P coda and Lg measurements at NORSAR, In: Semiann. Tech. Summ., 1 Apr - 30 Sep 1987, NORSAR Sci. Rep. 1-87/88, Kjeller, Norway.

Ringdal, F. and J. Fyen (1988): Comparative analysis of NORSAR and Gräfenberg Lg magnitudes of Shagan River explosions, In: Semiann. Tech. Summ., 1 Apr - 30 Sep 1988, NORSAR Sci. Rep. 1-88/89, Kjeller, Norway.

Stewart, R.C. (1988): P-wave seismograms from underground explosions at the Shagan River test site recorded at four arrays, AWE Report 0 4/88, HMSO, London.

Stimpson, I.G. (1988): Source parameters of explosions in granite at the French test site in Algeria, AWE Report 0 11/88, HMSO, London.

Storey, W.H., D.D. Eilers, T.O. McKown, D.M. Holt and G.C. Conrad (1982): CORRTEX-II, A dual microprocessor-controlled instrument for dynamic shock position measurements, Los Alamos National Laboratory Report LA-UR-82-558.

Sukhorukov, A.A., K.S. Akhmetov and I.V. Orlov (1973): Jubilee deposit, In: Geology of Coal and Oil Shale Deposits of the USSR, 217-230, Nedra, Moscow.

Sykes, L.R. and G. Ekström (1989): Comparison of seismic and hydrodynamic yield determinations for the Soviet Joint Verification Experiment of 1988, Proc. Natl. Acad. of Sci., USA, 86, 3456-3460.

No.	ORIGIN DATE	ORIGIN TIME	LAT	LON	MB	LOG RDP	N	STD	*** NORSAR **** M(LG)	N	STD	***** GRF ***** M(LG)	N	STD	FINAL M(LG)	SUB-REGION
1	01/15/65	5 59 58.4	49.940N	79.010E	5.870	3.87	1	0.14	-	-	-	-	-	-	-	TZ
2	06/19/68	5 05 57.3	49.982N	79.003E	5.280	3.31	4	0.07	-	-	-	-	-	-	-	NE
3	11/30/69	3 32 57.1	49.913N	78.961E	6.020	4.00	2	0.10	-	-	-	-	-	-	-	TZ
4	06/30/71	3 56 57.4	49.949N	78.986E	4.940	2.98	4	0.07	-	-	-	-	-	-	-	TZ
5	02/10/72	5 02 57.5	50.014N	78.878E	5.270	3.22	2	0.10	-	-	-	-	-	-	-	NE
6	11/02/72	1 26 57.6	49.923N	78.815E	6.160	4.38	1	0.14	6.118	42	0.014	-	-	-	6.118	SW
7	12/10/72	4 27 07.3	50.001N	78.973E	5.960	4.36	2	0.10	6.116	42	0.009	-	-	-	6.116	NE
8	07/23/73	1 22 57.6	49.962N	78.812E	6.170	-	-	-	6.199	40	0.006	-	-	-	6.199	TZ
9	12/14/73	7 46 57.2	50.044N	78.987E	5.790	3.84	1	0.14	5.868	42	0.033	-	-	-	5.868	NE
10	04/16/74	5 52 57.4	50.041N	78.943E	4.350	2.25	1	0.14	-	-	-	-	-	-	-	NE
11	05/31/74	3 26 57.5	49.950N	78.852E	5.810	3.88	1	0.14	-	-	-	-	-	-	-	TZ
12	10/16/74	6 32 57.6	49.979N	78.898E	5.410	3.17	3	0.08	5.411	42	0.024	-	-	-	5.411	TZ
13	12/27/74	5 46 56.9	49.943N	79.011E	5.500	3.07	3	0.08	5.708	42	0.056	-	-	-	5.708	NE
14	04/27/75	5 36 57.3	49.949N	78.926E	5.510	3.55	3	0.08	5.547	42	0.057	-	-	-	5.547	TZ
15	06/30/75	3 26 57.6	50.004N	78.957E	4.520	2.40	3	0.08	-	-	-	-	-	-	-	NE
16	10/29/75	4 46 57.3	49.946N	78.878E	5.610	3.42	4	0.07	5.629	42	0.046	-	-	-	5.629	TZ
17	12/25/75	5 16 57.2	50.044N	78.814E	5.690	3.59	4	0.07	5.801	42	0.035	-	-	-	5.801	NE
18	04/21/76	5 02 57.2	49.890N	78.827E	5.120	3.02	3	0.08	-	-	-	-	-	-	-	SW
19	06/09/76	3 02 57.2	49.989N	79.022E	5.070	3.08	3	0.08	5.199	42	0.089	-	-	-	5.199	NE
20	07/04/76	2 56 57.5	49.909N	78.911E	5.850	3.89	1	0.14	5.810	42	0.009	5.783	4	0.024	5.810	SW
21	08/28/76	2 56 57.5	49.969N	78.930E	5.740	3.68	3	0.08	5.735	41	0.013	5.653	3	0.052	5.733	TZ
22	11/23/76	5 02 57.3	50.008N	78.963E	5.790	3.81	3	0.08	-	-	-	5.792	3	0.057	5.819	NE
23	12/07/76	4 56 57.4	49.922N	78.846E	5.800	3.80	2	0.10	-	-	-	5.702	3	0.088	5.741	SW
24	05/29/77	2 56 57.6	49.937N	78.770E	5.750	3.80	1	0.14	5.677	41	0.035	5.573	3	0.038	5.655	SW
25	06/29/77	3 06 58.8	50.006N	78.869E	5.200	3.04	4	0.07	5.077	40	0.091	-	-	-	5.077	NE
26	09/05/77	3 02 57.3	50.035N	78.921E	5.730	3.93	3	0.08	5.897	40	0.017	5.769	3	0.036	5.879	NE
27	10/29/77	3 07 02.5	50.069N	78.975E	5.560	3.75	3	0.08	5.792	41	0.043	5.685	3	0.041	5.757	NE
28	11/30/77	4 06 57.4	49.958N	78.885E	5.890	3.92	2	0.10	-	-	-	5.716	3	0.041	5.753	TZ
29	06/11/78	2 56 57.6	49.898N	78.797E	5.830	3.87	4	0.07	5.752	39	0.029	5.724	4	0.039	5.755	SW
30	07/05/78	2 46 57.5	49.887N	78.871E	5.770	3.82	4	0.07	5.794	39	0.010	-	-	-	5.794	SW
31	08/29/78	2 37 06.3	50.000N	78.978E	5.900	3.98	4	0.07	6.010	39	0.008	6.010	6	0.022	6.010	NE
32	09/15/78	2 36 57.4	49.916N	78.879E	5.890	3.96	3	0.08	5.908	38	0.018	-	-	-	5.908	SW
33	11/04/78	5 05 57.3	50.034N	78.943E	5.560	3.66	4	0.07	5.697	39	0.080	5.636	6	0.080	5.690	NE
34	11/29/78	4 33 02.5	49.949N	78.798E	5.960	4.08	3	0.08	5.973	39	0.013	5.886	2	0.075	5.971	SW
35	02/01/79	4 12 57.6	50.090N	78.870E	5.290	3.30	3	0.08	-	-	-	-	-	-	-	NE
36	06/23/79	2 56 57.5	49.903N	78.855E	6.160	4.08	3	0.08	6.056	21	0.009	6.123	4	0.021	6.064	SW
37	07/07/79	3 46 57.3	50.026N	78.991E	5.840	3.73	3	0.08	5.969	38	0.008	5.938	7	0.021	5.966	NE
38	08/04/79	3 56 57.1	49.894N	78.904E	6.130	4.13	4	0.07	6.099	39	0.008	6.117	9	0.015	6.100	SW
39	08/18/79	2 51 57.1	49.943N	78.938E	6.130	4.13	4	0.07	-	-	-	6.145	7	0.017	6.126	TZ
40	10/28/79	3 16 56.9	49.973N	78.997E	5.980	3.92	2	0.10	6.053	34	0.010	6.046	8	0.023	6.051	NE
41	12/02/79	4 36 57.5	49.891N	78.796E	5.990	3.84	2	0.10	5.917	28	0.021	5.938	11	0.025	5.929	SW
42	12/23/79	4 56 57.4	49.916N	78.755E	6.130	3.92	1	0.14	-	-	-	6.045	9	0.021	6.039	SW
43	04/25/80	3 56 57.5	49.973N	78.755E	5.450	3.46	3	0.08	-	-	-	-	-	-	-	SW
44	06/12/80	3 26 57.6	49.980N	79.001E	5.520	3.55	3	0.08	-	-	-	5.571	11	0.105	5.627	NE
45	06/29/80	2 32 57.7	49.939N	78.815E	5.690	3.71	4	0.07	5.683	16	0.026	5.746	8	0.046	5.706	SW
46	09/14/80	2 42 39.1	49.921N	78.802E	6.210	4.36	1	0.14	-	-	-	-	-	-	-	SW
47	10/12/80	3 34 14.1	49.961N	79.028E	5.880	3.95	4	0.07	5.925	28	0.013	5.933	13	0.034	5.927	NE
48	12/14/80	3 47 06.4	49.899N	78.938E	5.930	3.98	4	0.07	5.929	28	0.018	5.944	10	0.027	5.936	TZ

Table VII.1.1. List of presumed explosions from the Shagan River area used in this study. The table includes, for each event, date, origin time, latitude, longitude, m_b (maximum likelihood), log Ψ_∞ (with number of stations and standard deviation of estimate), NORSAR and Gräfenberg M_{Lg} (including number of available channels and estimated precision of measurement), a weighted average of M_{Lg}, adjusted to NORSAR M_{Lg} scale and a region identifier. (Page 1 of 2)

No.	ORIGIN DATE	ORIGIN TIME	LAT	LON	MB	LOG RDP	N	STD	*** NORSAR **** M(LG)	N	STD	***** GRF ***** M(LG)	N	STD	FINAL M(LG)	SUB-REGION
49	12/27/80	4 9 8.1	50.057N	78.981E	5.870	3.89	3	0.08	5.939	27	0.014	5.885	11	0.034	5.933	NE
50	03/29/81	4 03 50.0	50.007N	78.982E	5.490	3.38	3	0.08	5.556	28	0.085	5.437	11	0.184	5.548	NE
51	04/22/81	1 17 11.3	49.885N	78.810E	5.940	4.07	3	0.08	5.908	28	0.022	5.956	11	0.027	5.929	SW
52	05/27/81	3 58 12.3	49.985N	78.980E	5.300	3.32	4	0.07	5.456	27	0.015	-	-	-	5.456	NE
53	09/13/81	2 17 18.3	49.910N	78.915E	6.060	4.18	4	0.07	6.113	29	0.008	6.106	9	0.015	6.108	TZ
54	10/18/81	3 57 02.6	49.923N	78.859E	6.000	4.05	4	0.07	5.985	34	0.010	5.956	9	0.021	5.981	SW
55	11/29/81	3 35 08.6	49.887N	78.860E	5.620	3.53	4	0.07	5.581	28	0.102	5.511	12	0.192	5.580	SW
56	12/27/81	3 43 14.1	49.923N	78.795E	6.160	4.19	2	0.10	6.074	34	0.009	6.092	10	0.020	6.075	SW
57	04/25/82	3 23 05.4	49.903N	78.913E	6.030	4.16	2	0.10	6.077	35	0.008	6.058	11	0.017	6.072	TZ
58	07/04/82	1 17 14.2	49.960N	78.807E	6.080	4.24	2	0.10	-	-	-	-	-	-	-	SW
59	08/31/82	1 31 00.7	49.924N	78.761E	5.200	3.03	4	0.07	-	-	-	-	-	-	-	SW
60	12/05/82	3 37 12.6	49.919N	78.813E	6.080	4.01	3	0.08	5.990	31	0.019	6.002	13	0.020	5.996	SW
61	12/26/82	3 35 14.2	50.071N	78.988E	5.580	3.60	4	0.07	5.658	39	0.050	5.597	13	0.067	5.655	NE
62	06/12/83	2 36 43.5	49.913N	78.916E	6.020	-	-	-	6.072	25	0.009	-	-	-	6.072	TZ
63	10/06/83	1 47 06.5	49.916N	78.764E	5.950	-	-	-	5.870	19	0.033	5.843	13	0.043	5.868	SW
64	10/26/83	1 55 04.8	49.901N	78.828E	6.040	3.92	3	0.08	6.000	33	0.021	6.036	13	0.021	6.016	SW
65	11/20/83	3 27 04.4	50.047N	78.999E	5.330	3.44	1	0.14	5.409	30	0.170	-	-	-	5.409	NE
66	02/19/84	3 57 03.4	49.885N	78.745E	5.770	3.71	3	0.08	5.725	29	0.038	-	-	-	5.725	SW
67	03/07/84	2 39 06.4	50.049N	78.954E	5.560	3.56	1	0.14	5.698	29	0.065	5.575	12	0.108	5.680	NE
68	03/29/84	5 19 08.2	49.912N	78.955E	5.860	3.73	1	0.14	5.897	29	0.012	5.957	13	0.043	5.902	TZ
69	04/25/84	1 09 03.5	49.929N	78.870E	5.900	-	-	-	5.870	35	0.008	5.803	13	0.031	5.867	SW
70	05/26/84	3 13 12.4	49.969N	79.006E	6.010	4.10	3	0.08	6.072	33	0.007	6.128	13	0.015	6.079	NE
71	07/14/84	1 09 10.5	49.893N	78.884E	6.100	3.97	1	0.14	6.054	32	0.007	6.064	12	0.015	6.054	SW
72	09/15/84	6 15 10.1	49.985N	78.883E	5.040	-	-	-	-	-	-	-	-	-	-	SW
73	10/27/84	1 50 10.6	49.920N	78.777E	6.190	4.13	3	0.08	6.085	33	0.011	6.145	13	0.016	6.098	SW
74	12/02/84	3 19 06.3	49.989N	79.011E	5.770	3.80	2	0.10	5.880	29	0.020	5.860	12	0.036	5.880	NE
75	12/16/84	3 55 02.7	49.926N	78.820E	6.120	4.06	2	0.10	6.048	29	0.010	6.038	13	0.014	6.043	SW
76	12/28/84	3 50 10.7	49.866N	78.703E	6.000	4.00	3	0.08	5.985	35	0.009	5.947	13	0.021	5.980	SW
77	02/10/85	3 27 07.5	49.888N	78.781E	5.830	3.82	4	0.07	5.803	40	0.024	5.801	13	0.058	5.806	SW
78	04/25/85	0 57 06.5	49.914N	78.902E	5.840	3.65	2	0.10	5.858	29	0.045	5.838	9	0.047	5.859	TZ
79	06/15/85	0 57 00.7	49.898N	78.845E	6.050	3.99	1	0.14	5.976	30	0.009	6.031	13	0.017	5.987	SW
80	06/30/85	2 39 02.6	49.848N	78.658E	5.920	3.95	2	0.10	5.931	30	0.009	5.906	13	0.017	5.928	SW
81	07/20/85	0 53 14.4	49.936N	78.785E	5.890	3.86	2	0.10	5.861	37	0.013	5.870	12	0.031	5.865	SW
82	03/12/87	1 57 17.2	49.939N	78.823E	5.310	3.28	4	0.07	5.218	33	0.076	-	-	-	5.218	SW
83	04/03/87	1 17 08.0	49.928N	78.829E	6.120	4.07	4	0.07	6.052	33	0.008	6.127	11	0.017	6.063	SW
84	04/17/87	1 03 04.8	49.886N	78.691E	5.920	4.00	4	0.07	5.901	33	0.020	5.915	12	0.026	5.910	SW
85	06/20/87	0 53 04.8	49.913N	78.735E	6.030	4.00	3	0.08	5.972	36	0.007	5.947	10	0.028	5.971	SW
86	08/02/87	0 58 06.8	49.880N	78.917E	5.830	3.97	3	0.08	5.871	30	0.011	5.853	11	0.022	5.871	SW
87	11/15/87	3 31 06.7	49.871N	78.791E	5.980	4.02	4	0.07	5.974	37	0.008	5.984	13	0.022	5.975	SW
88	12/13/87	3 21 04.8	49.989N	78.844E	6.060	4.17	2	0.10	6.093	31	0.010	6.067	12	0.015	6.082	SW
89	12/27/87	3 05 04.7	49.864N	78.758E	6.000	4.08	2	0.10	6.046	31	0.011	6.033	13	0.019	6.042	SW
90	02/13/88	3 05 05.9	49.954N	78.910E	5.970	4.01	3	0.08	6.042	26	0.009	6.045	13	0.029	6.042	TZ
91	04/03/88	1 33 05.8	49.917N	78.945E	5.990	4.15	2	0.10	6.063	31	0.007	6.071	13	0.014	6.063	TZ
92	05/04/88	0 57 06.8	49.928N	78.769E	6.090	4.06	3	0.08	6.044	31	0.008	6.068	13	0.020	6.046	SW
93	06/14/88	2 27 06.4	50.045N	79.005E	4.800	2.55	2	0.10	-	-	-	-	-	-	-	NE
94	09/14/88	4 00 00.0	49.870N	78.820E	6.030	4.05	2	0.10	5.969	37	0.010	5.970	12	0.043	5.969	SW
95	11/12/88	3 30 03.8	50.056N	78.991E	5.200	-	-	-	-	-	-	-	-	-	-	NE
96	12/17/88	4 18 06.8	49.818N	78.910E	5.800	-	-	-	5.801	37	0.018	-	-	-	5.801	TZ

Table VII.1.1. (Page 2 of 2)

EVENT NO	DATE	REG	ESTIMATED YIELDS LG	P	COMB
1	01/15/65	TZ	-	-	111*)
2	06/19/68	NE	-	26	26
3	11/30/69	TZ	-	135	135
4	06/30/71	TZ	-	9	9
5	02/10/72	NE	-	24	24
6	11/02/72	SW	166	168	167
7	12/10/72	NE	165	159	162
8	07/23/73	TZ	204	200	202
9	12/14/73	NE	88	93	90
10	04/16/74	NE	-	2	2
11	05/31/74	TZ	-	81	81
12	10/16/74	TZ	27	26	27
13	12/27/74	NE	58	36	46
14	04/27/75	TZ	39	39	39
15	06/30/75	NE	-	4	4
16	10/29/75	TZ	47	44	46
17	12/25/75	NE	74	66	70
18	04/21/76	SW	-	11	11
19	06/09/76	NE	16	15	15
20	07/04/76	SW	76	74	75
21	08/28/76	TZ	62	66	64
22	11/23/76	NE	77	91	84
23	12/07/76	SW	63	65	64
24	05/29/77	SW	51	58	54
25	06/29/77	NE	12	19	15
26	09/05/77	NE	90	85	88
27	10/29/77	NE	66	55	60
28	11/30/77	TZ	65	99	80
29	06/11/78	SW	66	72	69
30	07/05/78	SW	72	62	67
31	08/29/78	NE	126	123	125
32	09/15/78	SW	97	85	91
33	11/04/78	NE	56	53	54
34	11/29/78	SW	114	103	108
35	02/01/79	NE	-	26	26
36	06/23/79	SW	145	155	150
37	07/07/79	NE	113	97	105
38	08/04/79	SW	158	149	154
39	08/18/79	TZ	169	180	174
40	10/28/79	NE	140	144	142
41	12/02/79	SW	102	100	101
42	12/23/79	SW	136	145	140
43	04/25/80	SW	-	27	27
44	06/12/80	NE	47	46	47
45	06/29/80	SW	58	50	54
46	09/14/80	SW	-	189	189
47	10/12/80	NE	102	117	109
48	12/14/80	TZ	104	112	108

Table VII.1.2. Estimated yields for the explosions of Table VII.1.1, as discussed in the text. For each event (except for Event 1, see text), we list a) yield estimate based on Lg waves (NORSAR and GRF), b) yield estimate based on P waves (m_b and log Ψ_∞) and c) a combined estimate, obtained by logarithmic averaging of a) and b). (Page 1 of 2)

EVENT			ESTIMATED YIELDS		
NO	DATE	REG	LG	P	COMB
49	12/27/80	NE	103	111	107
50	03/29/81	NE	39	40	40
51	04/22/81	SW	102	98	100
52	05/27/81	NE	31	27	29
53	09/13/81	TZ	162	161	162
54	10/18/81	SW	117	111	114
55	11/29/81	SW	42	40	41
56	12/27/81	SW	149	163	156
57	04/25/82	TZ	148	146	147
58	07/04/82	SW	-	139	139
59	08/31/82	SW	-	13	13
60	12/05/82	SW	121	128	124
61	12/26/82	NE	51	54	52
62	06/12/83	TZ	148	136	142
63	10/06/83	SW	87	95	91
64	10/26/83	SW	128	113	120
65	11/20/83	NE	27	29	28
66	02/19/84	SW	61	59	60
67	03/07/84	NE	54	51	53
68	03/29/84	TZ	95	89	92
69	04/25/84	SW	87	84	85
70	05/26/84	NE	150	163	157
71	07/14/84	SW	141	136	138
72	09/15/84	SW	-	9	9
73	10/27/84	SW	158	169	163
74	12/02/84	NE	90	87	89
75	12/16/84	SW	137	143	140
76	12/28/84	SW	117	108	112
77	02/10/85	SW	75	70	72
78	04/25/85	TZ	85	81	83
79	06/15/85	SW	119	121	120
80	06/30/85	SW	102	89	95
81	07/20/85	SW	87	81	84
82	03/12/87	SW	17	19	18
83	04/03/87	SW	144	141	143
84	04/17/87	SW	98	92	95
85	06/20/87	SW	114	115	114
86	08/02/87	SW	88	75	81
87	11/15/87	SW	115	105	110
88	12/13/87	SW	151	130	140
89	12/27/87	SW	137	111	123
90	02/13/88	TZ	137	123	129
91	04/03/88	TZ	144	133	138
92	05/04/88	SW	138	133	136
93	06/14/88	NE	-	7	7
94	09/14/88	SW	113	117	115
95	11/12/88	NE	-	20	20
96	12/17/88	TZ	74	77	76

Table VII.1.2. (Page 2 of 2)

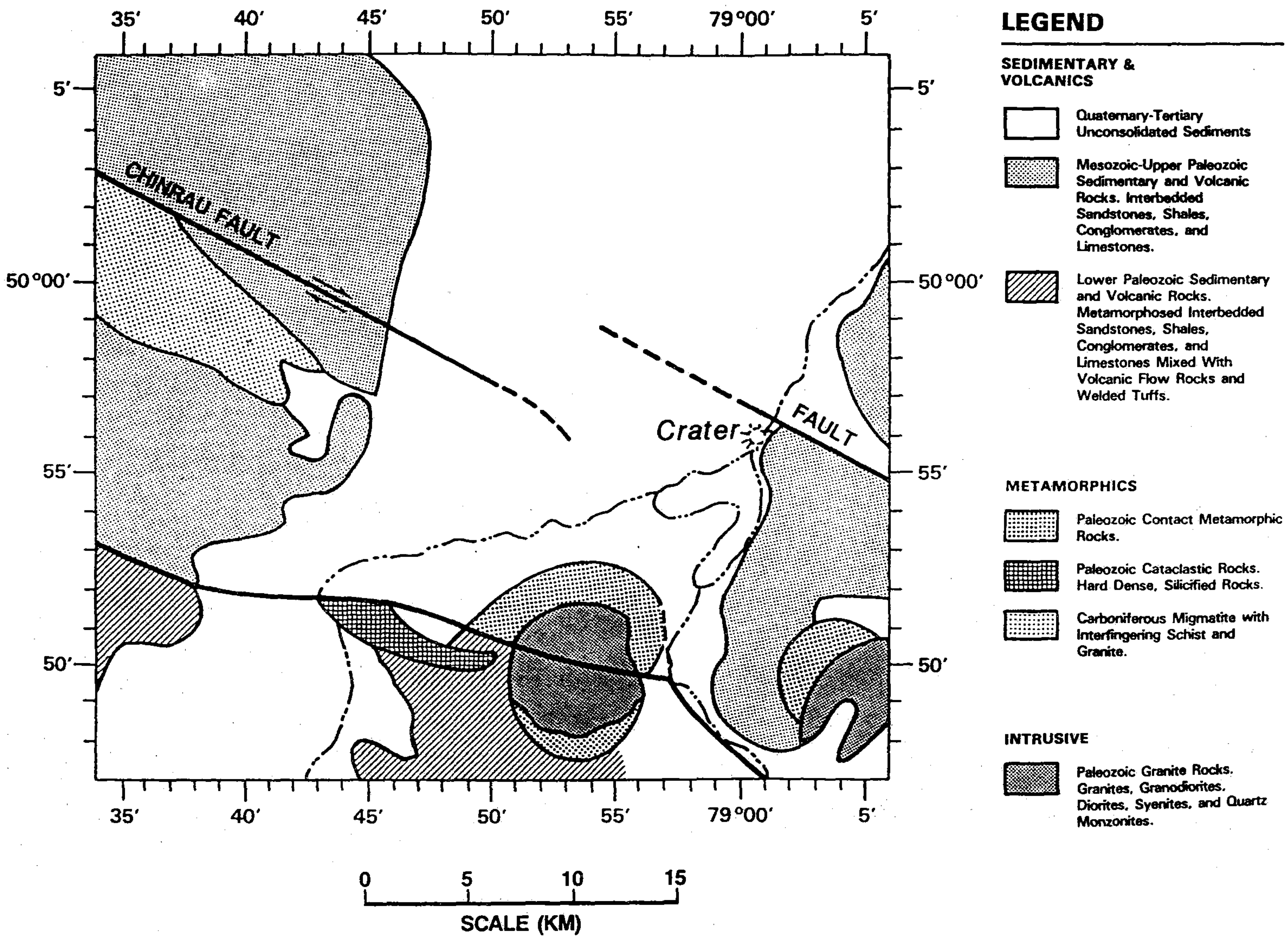

Fig. VII.1.1. Surface geology of the Shagan River area. The crater from the 15 January 1965 explosion is indicated. Note the two faults marked on the figure.

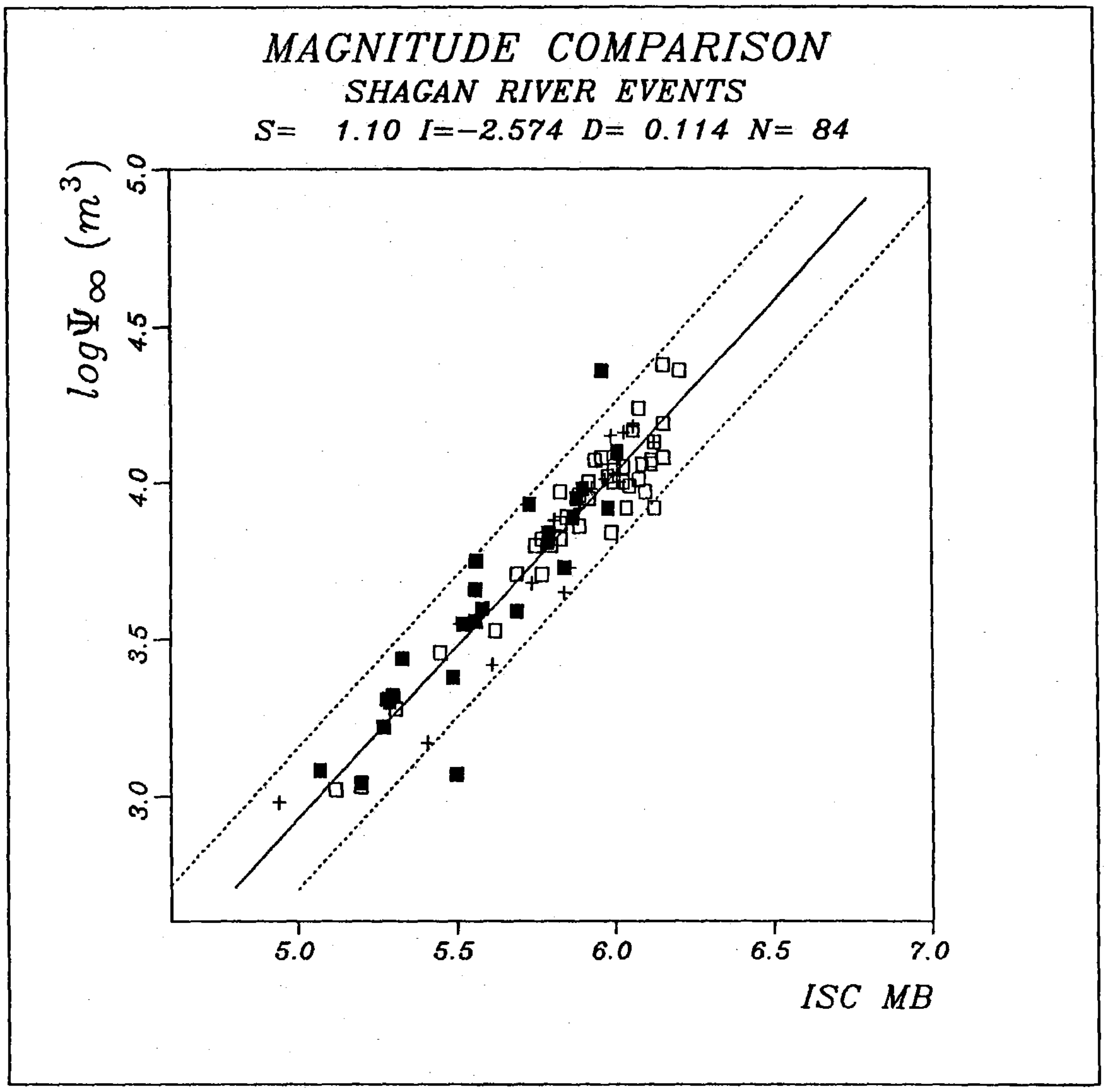

Fig. VII.1.2. Array network log Ψ_∞ plotted against maximum likelihood m_b. Open and filled symbols denote SW and NE events, respectively, whereas crosses denote TZ events. The line drawn through the data is the best least squares straight line, assuming no error in m_b. The dotted lines correspond to plus/minus two standard deviations in the vertical direction.

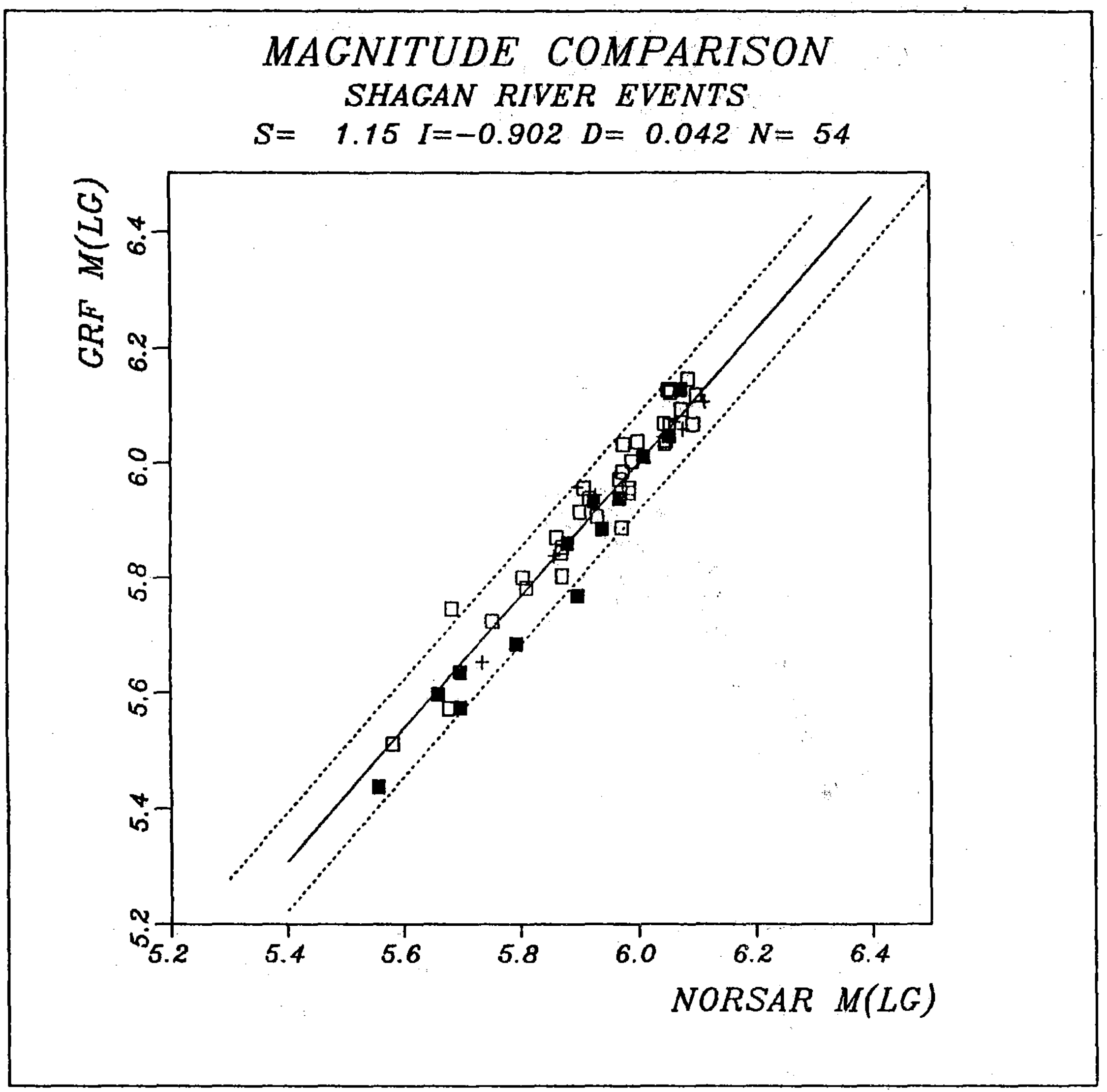

Fig. VII.1.3. Gräfenberg m_{Lg} plotted against NORSAR m_{Lg}. The line drawn through the data is the best least squares fit, assuming no error in NORSAR m_{Lg}. The dotted lines correspond to plus/minus two standard deviations. Note the consistency between SW events (open symbols), NE events (filled symbols) and TZ events (crosses).

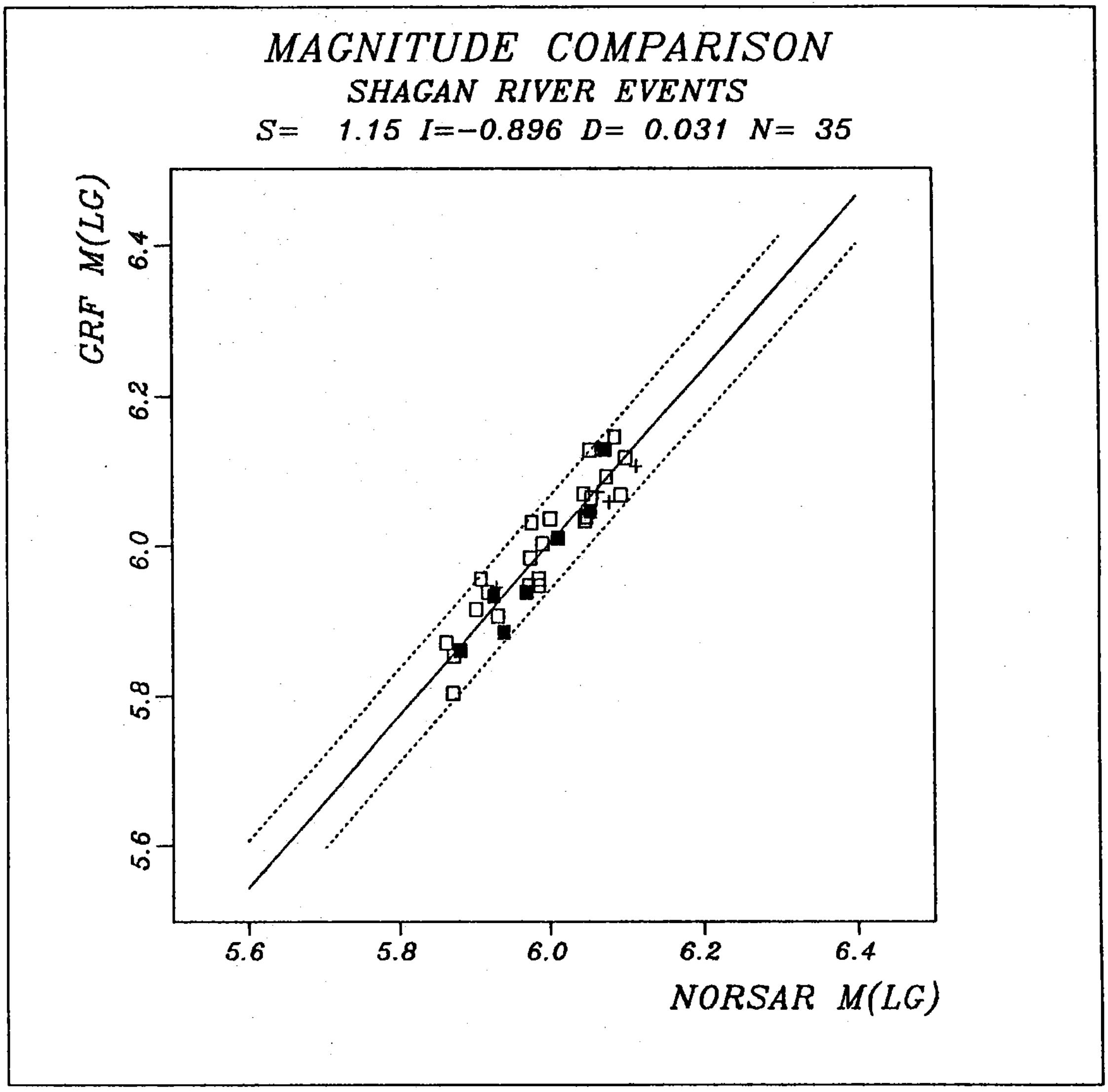

Fig. VII.1.4. Gräfenberg m_{Lg} plotted against NORSAR m_{Lg} for well-recorded events, i.e., requiring at least 6 sensors available, and a precision of measurement better than 0.04 for each array. Note the reduction in scatter compared to Fig. VII.1.3.

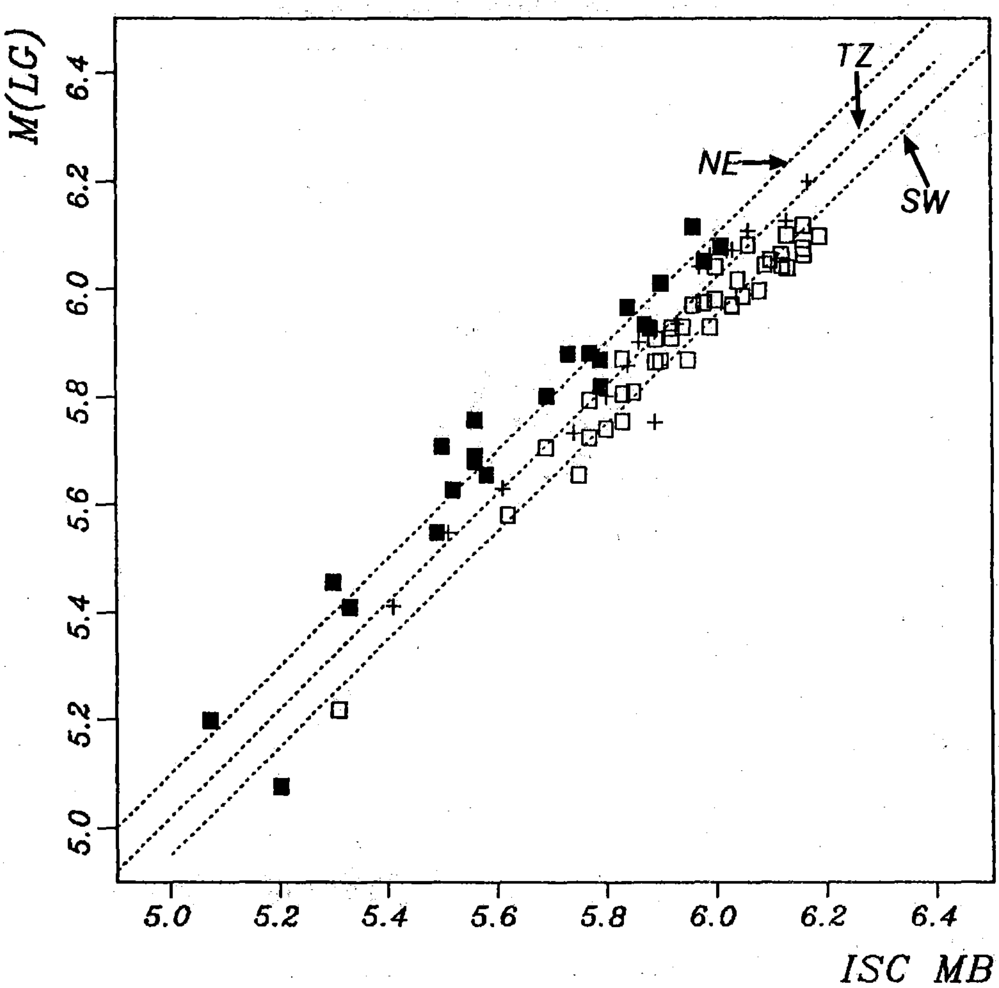

Fig. VII.1.5. NORSAR/GRF m_{Lg} plotted against maximum likelihood m_b. Note the difference between SW events (open symbols), NE events (filled symbols) and TZ events (crosses). A straight line has been fitted to each of these three subsets, with a slope restricted to 1.00.

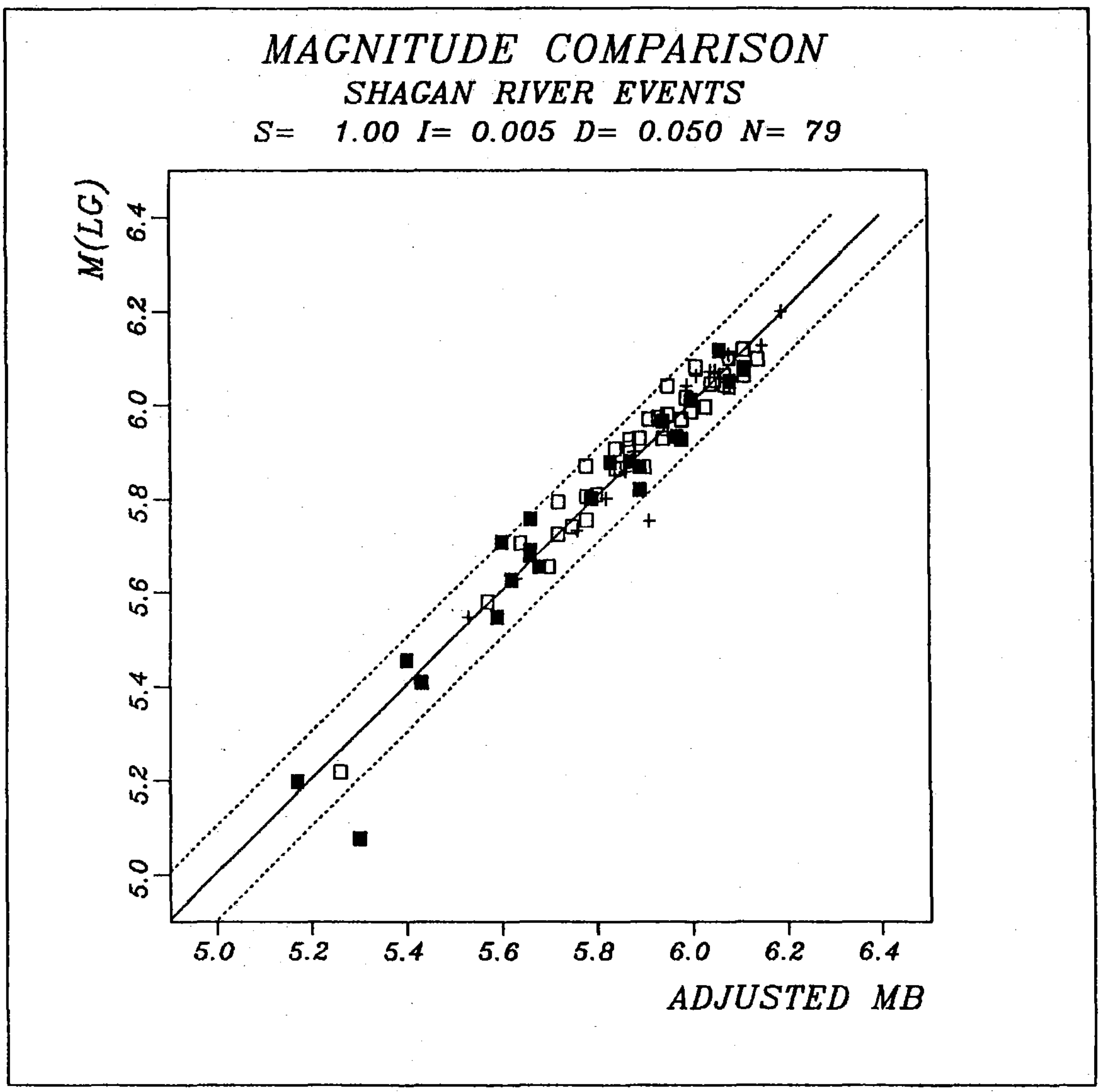

Fig. VII.1. 6. NORSAR/GRF m_{Lg} plotted against "adjusted m_b", i.e., m_b values adjusted for average bias in each of the three subregions. Note the excellent correspondence, with the exception of two outliers as discussed in the text.

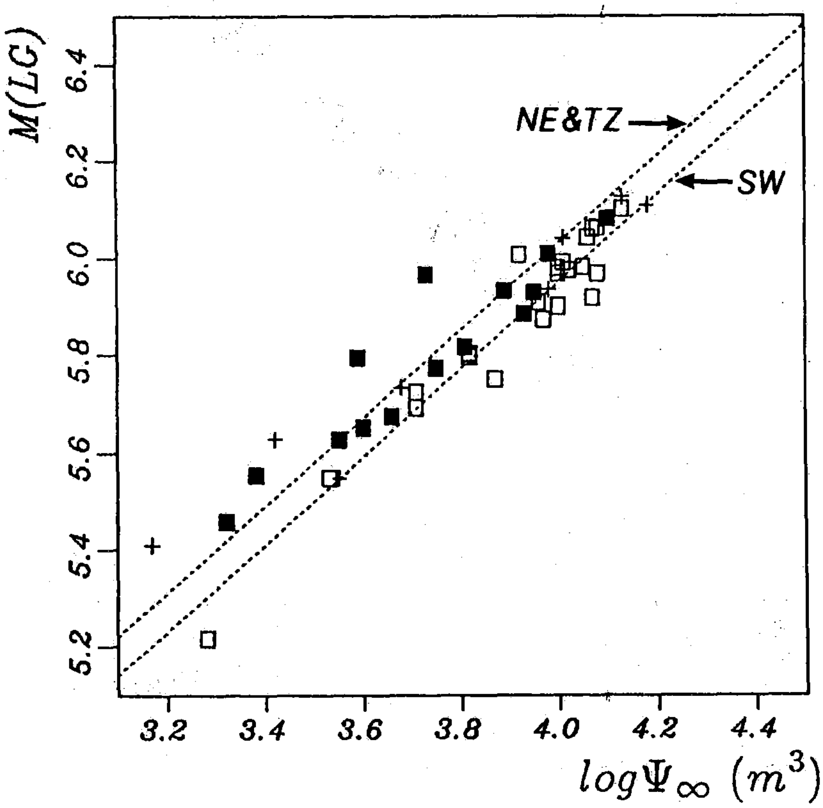

Fig. VII.1.7. NORSAR/GRF m_{Lg} plotted against network averaged log Ψ_∞, requiring at least three station observations for the latter. The two stippled lines (slope of 0.9) represent linear fits to the SW events and the NE/TZ events, respectively. Symbol conventions are as in Fig. VII.1.2.

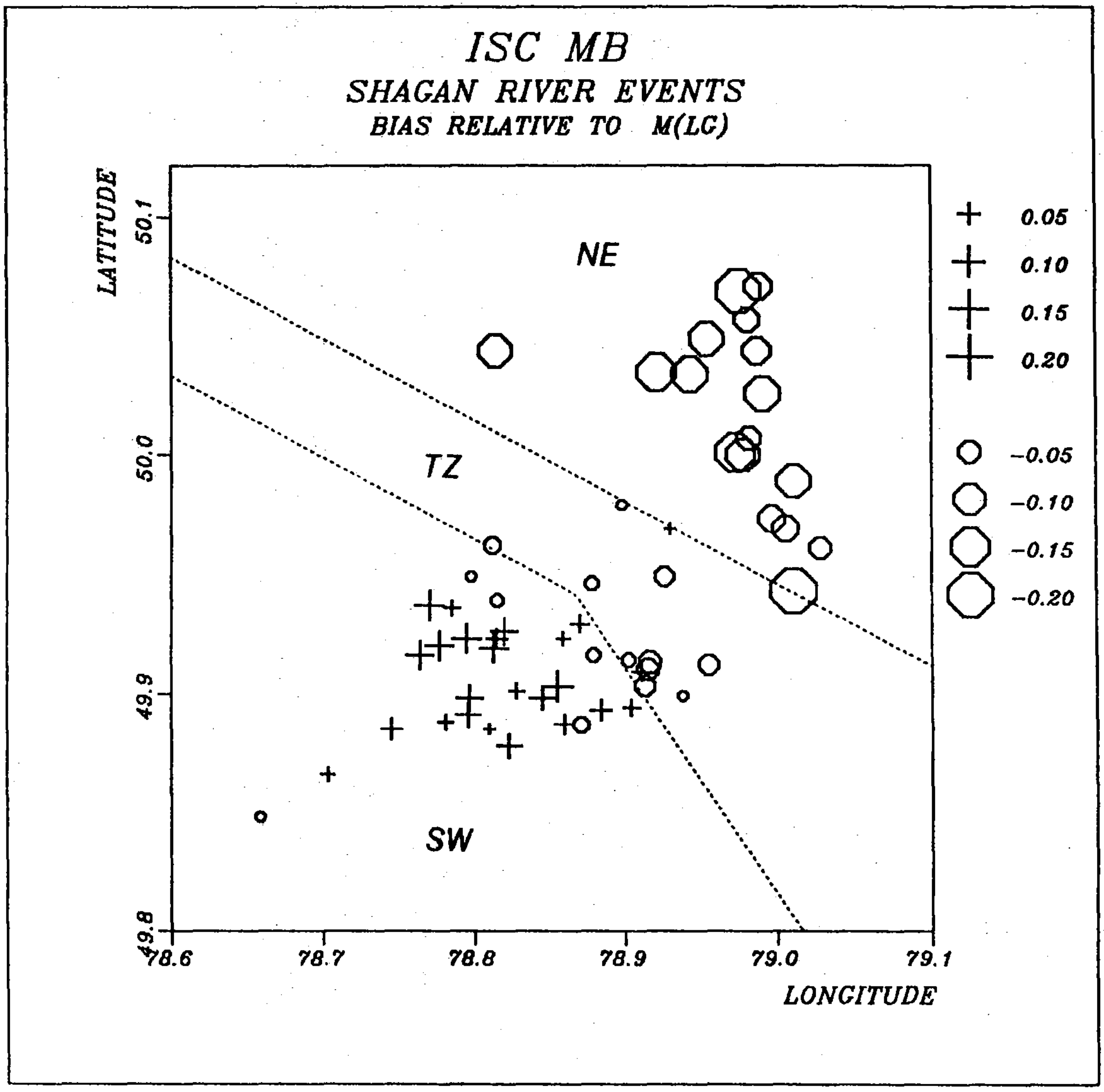

Fig. VII.1.8. Plot of magnitude residuals (maximum likelihood m_b minus m_{Lg}) as a function of event location for events of $m_b \geq 5.50$. Only events with NORSAR data available have been included. Plusses and circles correspond to residuals greater or less than zero, respectively, with symbol size proportional to the deviation. Location estimates are those in Table VII.1.1, and only events prior to 1986 (which have the most precise locations) have been included. Note the systematic variation within the Shagan River areas, with different patterns in the three subregions.